Acta Cryst E CRYSTALLOGRAPHIC COMMUNICATIONS

ISSN 2056-9890

Crystal structure of 1-(4-methylphenyl)-3-(propan-2-ylideneamino)thiourea

Mukesh M. Jotani,[a]‡ Chien Ing Yeo[b] and Edward R. T. Tiekink[b,c]*

[a]Department of Physics, Bhavan's Sheth R. A. College of Science, Ahmedabad, Gujarat 380001, India, [b]Department of Chemistry, University of Malaya, 50603 Kuala Lumpur, Malaysia, and [c]Centre for Chemical Crystallography, Faculty of Science and Technology, Sunway University, 47500 Bandar Sunway, Selangor Darul Ehsan, Malaysia. *Correspondence e-mail: edward.tiekink@gmail.com

Received 15 September 2015
Accepted 20 September 2015

Edited by W. T. A. Harrison, University of Aberdeen, Scotland

‡ Additional correspondence author, e-mail: mmjotani@rediffmail.com.

Keywords: crystal structure; hydrogen bonding; thiourea derivative; thiosemicarbazone; Hirshfeld surface analysis

CCDC reference: 1425975
Supporting information: this article has supporting information at journals.iucr.org/e

In the title thiosemicarbazone, $C_{11}H_{15}N_3S$, the *p*-tolyl-N—H and imino-N—H groups are *anti* and *syn*, respectively, to the central thione-S atom. This allows for the formation of an intramolecular *p*-tolyl-N—H···N(imino) hydrogen bond. The molecule is twisted with the dihedral angle between the *p*-tolyl ring and the non-hydrogen atoms of the N=CMe$_2$ residue being 29.27 (8)°. The crystal packing features supramolecular layers lying in the *bc* plane whereby centrosymmetric aggregates sustained by eight-membered thioamide $\{\cdots HNCS\}_2$ synthons are linked by further N—H···S hydrogen bonds. Layers are connected *via* methyl-C—H···π interactions. The supramolecular aggregation was further investigated by an analysis of the Hirshfeld surface and comparison made to related structures.

1. Chemical context

The reaction between an alcohol or amine (primary or secondary) with *N*-alkyl- or *N*-aryl-isothiocyanides usually results in the formation of thiocarbamides. For example, in the case of reactions involving a monofunctional alcohol, the reaction proceeds in the following manner: R—OH + R'N=C=S → ROC(=S)N(H)R' (Ho *et al.*, 2005). Often, reactions are facilitated by initially employing an alkali metal hydroxide as the base and later adding an acid, *e.g.* HCl (Ho *et al.*, 2005). Such molecules are of interest as when deprotonated, they can function as effective thiolate ligands for phosphanegold(I) derivatives, which display biological activity. For example, Ph$_3$PAu[SC(O–alkyl)=N(aryl)] compounds exhibit significant cytotoxicity against a variety of cancer cell lines and mechanistic studies show that they can kill cancer cells by initiating a variety of apoptotic pathways, both extrinsic and intrinsic (Yeo, Ooi *et al.*, 2013; Ooi, Yeo *et al.*, 2015). Related species, *i.e.* Ph$_3$PAu[SC(O–alkyl)=N(*p*-tolyl)], exhibit potency against Gram-positive bacteria (Yeo, Sim *et al.*, 2013). Over and above these considerations, systematic studies into the structural chemistry of these molecules, which have proven relatively easy to crystallize, have been of some interest in crystal engineering endeavours (Ho *et al.*, 2006; Kuan *et al.*, 2008). In the course of studies to increase the functionality of the thiocarbamide molecules, bipodal {1,4-[MeOC(=S)N(H)]$_2$C$_6$H$_4$} was successfully synthesized along with binuclear phosphanegold(I) complexes (Yeo, Khoo *et al.*, 2015). Recent attempts at expanding this chemistry by using thiourea as an amine donor have been undertaken. As reported very recently, 1:2 reactions between thiourea and R'N=C=S resulted in the isolation of salts containing 1,2,3-thiazole-based cations resulting from 1:1 cyclizations (Yeo, Tan *et al.*, 2015). Herein, the product of an analogous reaction

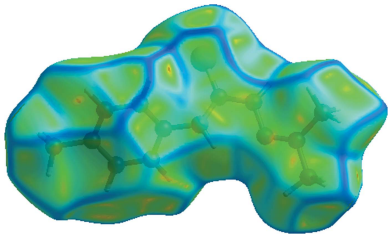

involving a bifunctional amine, *i.e.* H_2NNH_2 (hydrazine) with (*p*-tolyl)N═C═S, conducted in acetone solution, is described, namely the thiosemicarbazone, (I). Molecules related to (I) and especially their metal complexes continue to attract attention owing to potential biological activity (Dilworth & Hueting, 2012; Lukmantara *et al.*, 2013; Su *et al.*, 2013).

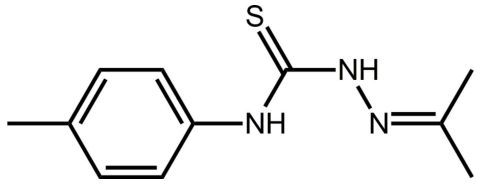

1.1. Structural commentary

The molecular structure of (I), Fig. 1, comprises three planar regions. The central NC(═S)N chromophore (the r.m.s. deviation of the fitted atoms is 0.0020 Å) has *anti*- and *syn*-dispositions of the N1- and N2-bound H atoms, respectively, with respect to the central thione-S1 atom. The N1-bound H atom is *syn* to the imino-N3 atom allowing for the formation of a five-membered loop *via* an N1—H···N3 hydrogen bond, Table 1. The central plane forms dihedral angles of 23.49 (4)° with the propan-2-ylideneamino residue (N═CMe_2; r.m.s. deviation for the C_3N atoms = 0.0002 Å) and 43.30 (5)° with the *p*-tolyl ring. Overall, the molecule is twisted as quantified by the dihedral angle between the outer planes of 29.27 (8)°.

Two $P2_1/c$ polymorphs have been reported for the parent compound, *i.e.* having a phenyl rather than a *p*-tolyl substituent (Jian *et al.*, 2005; Venkatraman *et al.*, 2005); the structure of (I) also crystallizes in the $P2_1/c$ space group. As revealed from the data collated in Table 2, there is a high degree of concordance in the key bond lengths and angles for the three molecules, as might be expected. However, there are some notable differences in the torsion-angle data as well as in the dihedral angles between the three least-squares planes discussed above, Table 2. From these and the overlay diagram shown in Fig. 2, it is apparent that the molecular structure of (I) more closely matches that observed in the polymorph reported by Venkatraman *et al.* (2005) rather than that described by Jian *et al.* (2005). This conclusion is also vindicated in the unit cell data, *i.e.* *a* = 12.225 (3), *b* = 7.618 (2), *c* = 11.639 (3) Å, *β* = 102.660 (4)° reported for the former (Venkatraman *et al.*, 2005).

Table 1
Hydrogen-bond geometry (Å, °).

*Cg*1 is the centroid of the C2–C7 ring.

D—H···*A*	*D*—H	H···*A*	*D*···*A*	*D*—H···*A*
N1—H1*N*···N3	0.88 (1)	2.09 (2)	2.572 (2)	114 (1)
N1—H1*N*···S1^{i}	0.88 (1)	2.87 (2)	3.5618 (17)	137 (2)
N2—H2*N*···S1^{ii}	0.88 (2)	2.57 (2)	3.4373 (16)	169 (2)
C8—H8*C*···*Cg*1^{iii}	0.98	2.81	3.716 (2)	154

Symmetry codes: (i) $x, -y+\frac{1}{2}, z-\frac{1}{2}$; (ii) $-x, -y, -z+1$; (iii) $-x+1, -y, -z+1$.

Table 2
Geometric data (Å, °) for (I) and two polymorphs of (II).

Parameter	(I)	Form *a* of (II)[a]	Form *b* of (II)[b]
N2—N3	1.397 (2)	1.386 (2)	1.392 (2)
C1—S1	1.6873 (18)	1.6816 (17)	1.6826 (17)
C1—N1	1.350 (2)	1.337 (2)	1.343 (2)
C1—N2	1.350 (2)	1.359 (2)	1.348 (2)
C2—N1	1.422 (2)	1.420 (2)	1.425 (2)
C9—N3	1.280 (2)	1.279 (2)	1.276 (2)
C1—N1—C2	127.79 (16)	129.98 (14)	127.97 (14)
C1—N2—N3	117.72 (15)	118.17 (14)	118.33 (14)
N2—N3—C9	117.91 (15)	118.85 (15)	117.73 (14)
S1—C1—N1	125.45 (14)	126.00 (13)	125.75 (13)
S1—C1—N2	120.00 (14)	119.37 (13)	119.50 (12)
N1—C1—N2	114.54 (16)	114.63 (15)	114.74 (15)
S1—C1—N2—N3	−169.57 (12)	177.46 (12)	−170.56 (12)
C1—N1—C2—C3	132.2 (2)	−153.87 (18)	131.10 (19)
C1—N2—N3—C9	−165.78 (16)	168.43 (16)	−165.85 (15)
CN_2S / C_3N	23.49 (4)	13.19 (8)	22.42 (9)
CN_2S / aryl	43.30 (5)	39.26 (6)	43.90 (6)
C_3N / aryl	29.27 (8)	40.15 (8)	30.18 (8)

Notes: (*a*) Jian *et al.* (2005); (*b*) Venkatraman *et al.* (2005).

2. NMR invesitgations

The conformation of (I) was also investigated in $CDCl_3$ solution by NMR methods. Assignments were made with the aid of the interpretative program, *Chemdraw Ultra* (CambridgeSoft Corporation, 2002). On the basis of multiple

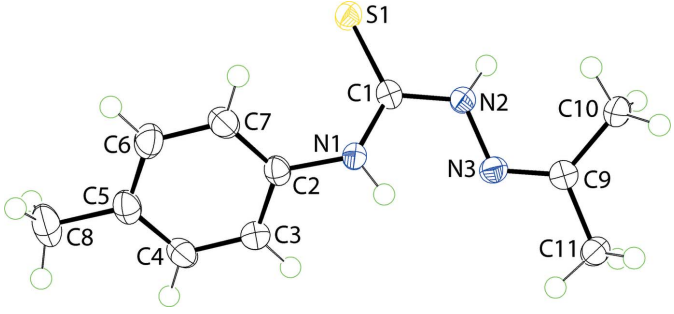

Figure 1
The molecular structure of (I) showing displacement ellipsoids at the 70% probability level.

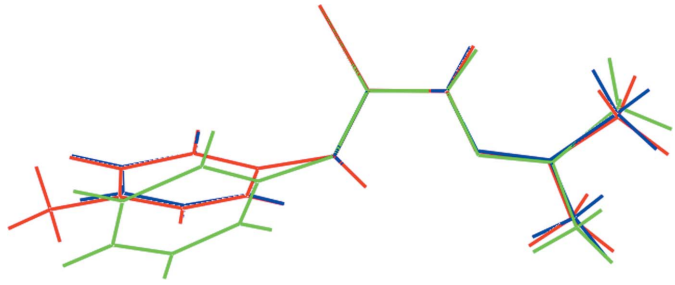

Figure 2
Overlay diagram of the molecules in (I), red image, and (II), forms *a* (green) and *b* (blue). The molecules have been overlapped so that the central NC(═S)N chromophores are coincident.

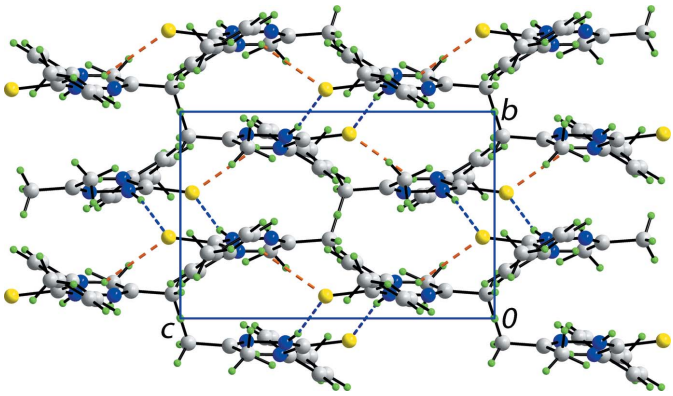

Figure 3
Supramolecular layer in the *bc* plane in the crystal packing of (I). Centrosymmetric aggregates mediated by eight-membered thioamide $\{\cdots HNCS\}_2$ synthons (shown as orange dashed lines) are linked by additional amide-N—H···S hydrogen bonds, shown as blue dashed lines.

^1H and $^{13}C\{^1H\}$ resonances for the methyl groups of the propan-2-ylideneamino residue, it appears that the (propan-2-ylideneamino)thiourea residue has a locked configuration, consistent with the persistence of the intramolecular N1—H···N3 hydrogen bond in $CDCl_3$ solution.

3. Supramolecular features

In the crystal, N—H···S and C—H···π interactions provide identifiable points of contact between molecules; these interactions are quantified in Table 1. Centrosymmetrically related molecules are connected by pairs of amide-N2—H···S1 hydrogen bonds, forming eight-membered thioamide $\{\cdots HNCS\}_2$ synthons. These are connected into supramolecular layers in the *bc* plane by amide-N1—H···S1 hydrogen bonds so that the S1 atom accepts two hydrogen bonds, Fig. 3. The *p*-tolyl groups protrude to either side of each layer and inter-digitate along the *a* axis with adjacent layers allowing for the formation of methyl-C8—H···π(C2–C7) interactions, thereby consolidating the three-dimensional architecture, Fig. 4.

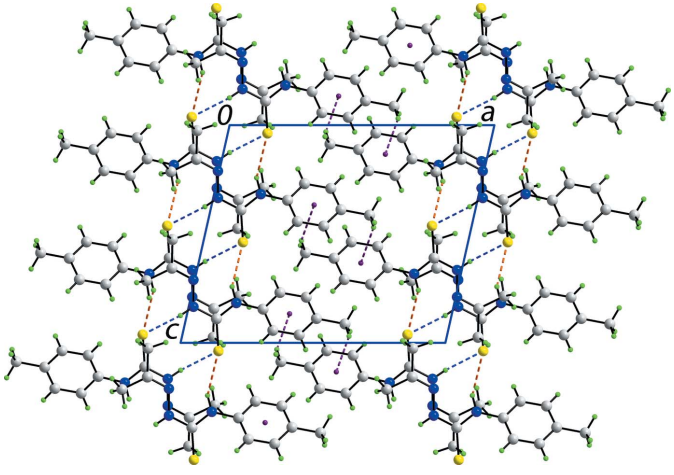

Figure 4
A view of the unit cell contents of (I) shown in projection down the *b* axis. Supramolecular layers, illustrated in Fig. 3, are linked *via* C—H···π interactions, shown as purple dashed lines, leading to a three-dimensional architecture.

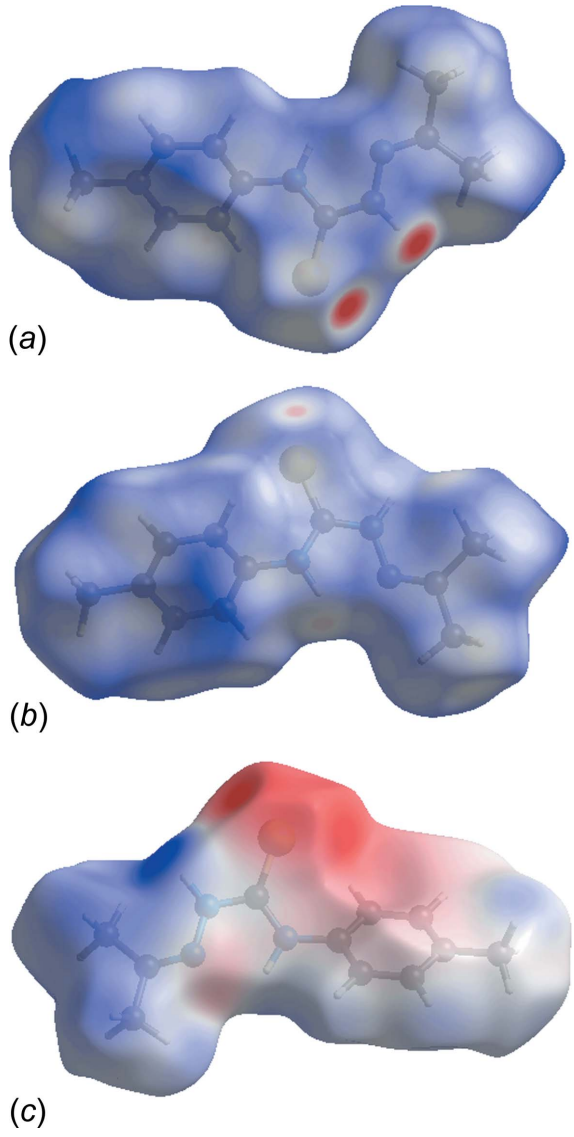

Figure 5
Views of the Hirshfeld surface for (I): (*a*) and (*b*) mapped over d_{norm}, and (*c*) mapped over the calculated electrostatic potential.

4. Analysis of the Hirshfeld surfaces

The crystal packing was further investigated by an analysis of the Hirshfeld surface (Spackman & Jayatilaka, 2009) employing *CrystalExplorer* (Wolff *et al.*, 2012). Fingerprint plots (Rohl *et al.*, 2008) were calculated, as were the electrostatic potentials using *TONTO* (Spackman *et al.*, 2008; Jayatilaka *et al.*, 2005) integrated into *CrystalExplorer*; the electrostatic potentials were mapped on the Hirshfeld surfaces using the STO–3G basis set at the level of Hartree–Fock theory over a range of ±0.075 au.

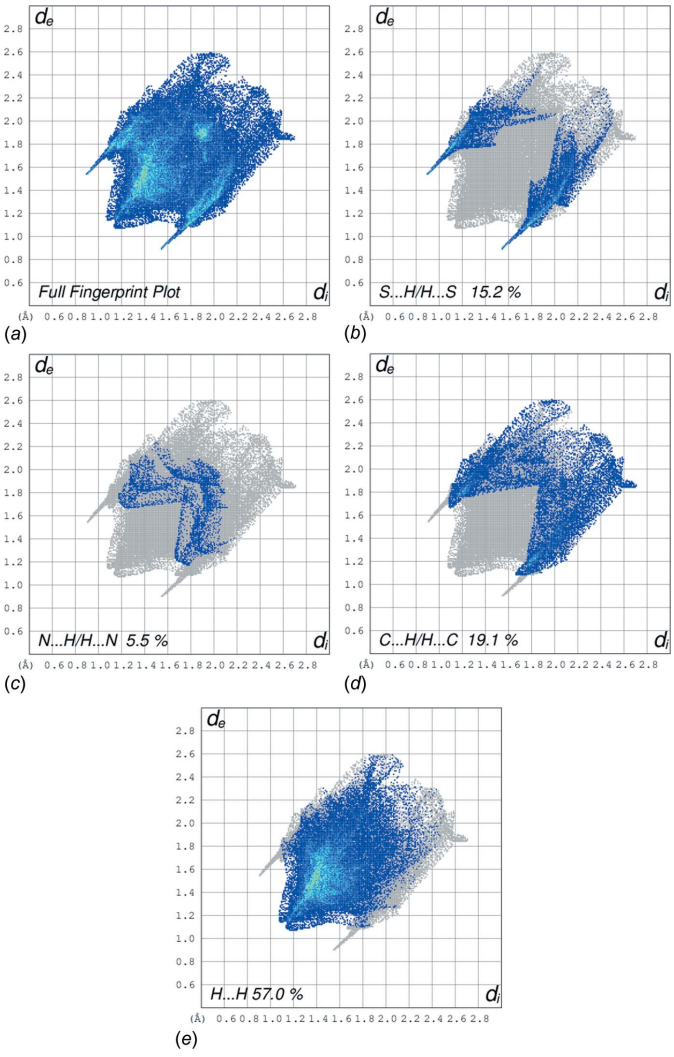

Figure 6
2D Fingerprint plots for (I): (*a*) full, (*b*) delineated to show S···H/H···S, (*c*) N···H/H···N, (*d*) C···H/H···C, and (*e*) H···H interactions.

Two views of the Hirshfeld surface mapped over d_{norm} are shown in Fig. 5*a* and *b*. The deep-red depressions at the S1 and N2 atoms (Fig. 5*a*) confirm their role as an acceptor and donor in the hydrogen-bonding scheme, respectively. This is also evident from the dark-red and blue regions, respectively, on the Hirshfeld surface mapped over the calculated electrostatic potential (Fig. 5*c*). The diminutive red spots near S1 and N1 (Fig. 5*b*) indicate their involvement in the intermolecular N—H···S hydrogen bond.

The overall two-dimensional fingerprint plot (Fig. 6*a*) and those delineated into H···H, S···H/H···S, N···H/H···N and C···H/H···C H···H (Fig. 6*b–d*, respectively) interactions operating in the crystal structure of (I) are illustrated in Fig. 6; the relative contributions are summarized in Table 3. The prominent pair of sharp spikes of equal length (d_e + d_i = 2.45 Å; Fig. 6*b*) with a 15.2% contribution due to S···H/H···S contacts to the Hirshfeld surfaces also suggest the presence of these interactions in the crystal packing. The light-red region near N3 (Fig. 5*a*) and diminutive red spot near N1—H (Fig. 5*b*) are consistent with relatively smaller contributions from

Table 3
Relative contribution (%) to intermolecular interactions calculated from the Hirshfeld surface.

Contact	Contribution
H···H	57.0
S···H/H···S	15.2
N···H/H···N	5.5
C···H/H···C	19.1
C···C	0.7
N···N	1.4
C···N	0.8
C···S	0.2
others	0.1

N···H/H···N contacts, *i.e.* 2.5 and 3.0%, respectively, and are indicative of the weak intramolecular hydrogen bond. The strength of such an interaction can be visualized from the 2D fingerprint plot corresponding to N···H/ H···N contacts (Fig. 6*c*). The bright-orange spot in the surface mapped with d_e (within a red circle in Fig. 7) about the aryl ring and a light-blue region around the tolyl-hydrogen atom, H8*C* (Fig. 7), suggest a contribution from the C—H···π interaction (Table 1). This is also evident through distinct pair of 'wings' in the fingerprint plot corresponding to C···H/H···C contacts (Fig. 6*d*). The wing at the top, left belongs to C—H donors, while that at the bottom, right corresponds to the surface around π-acceptors with 11.3 and 7.8% contribution from C···H and H···C contacts, respectively. The H···H contacts reflected in the middle of scattered points in Fig. 6*e* provide

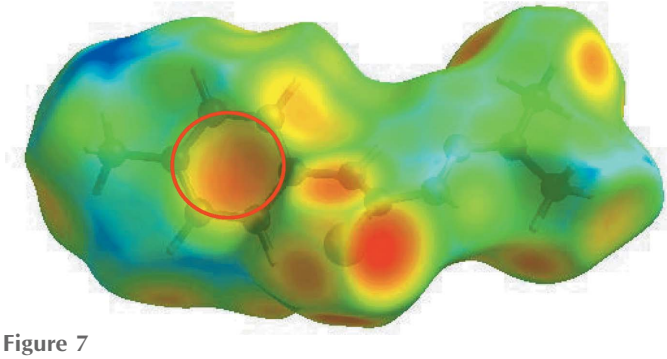

Figure 7
View of the Hirshfeld surface for (I) mapped over d_e.

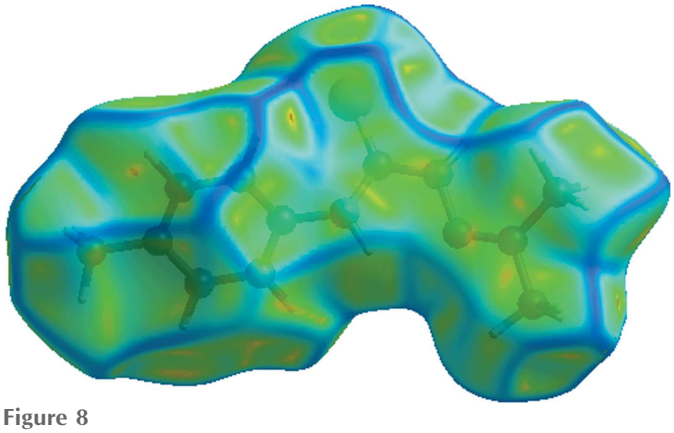

Figure 8
Hirshfeld surfaces for (I) mapped over curvedness.

the most significant contribution, *i.e.* 57.0%, to the Hirshfeld surface arising from a side-ways approach. The small, flat segments delineated by the blue outline in the surface mapped with curvedness (Fig. 8) and the small (*i.e.* 0.7%) contribution from C···C contacts to the surface indicates the absence of π–π stacking interactions in the structure.

5. Database survey

According to a search of the Cambridge Structural Database (Groom & Allen, 2014), there are no direct analogues of (I), either in the coordinated or uncoordinated form. As mentioned in the *Structural commentary*, the parent compound has been characterized in two polymorphic forms (Jian *et al.*, 2005; Venkatraman *et al.*, 2005). The parent compound, LH, has also been observed to coordinate metal centres. Thus, monodentate coordination *via* the thione-S atom was observed in a neutral complex $[ZnCl_2(LH)_2]$ (Bel'skii *et al.*, 1987). By contrast, a chelating mode *via* thione-S and imino-N atoms was observed in each of the charged complexes $[CoBr(LH)_2]Br$ (Dessy *et al.*, 1978) and $[(\eta^6$-*p*-cymene)RuCl(LH)]Cl (Su *et al.*, 2013). The most closely related structure having the *p*-tolyl substituent but variations at the imino-N atom is one where one methyl group has been substituted by a phenyl (Zhang *et al.*, 2011). This is also a twisted molecule with the dihedral angle between the *p*-tolyl and NC_3 residues being 65.44 (7)°.

6. Synthesis and crystallization

To *p*-tolyl isothiocyanate (Sigma–Aldrich; 10 mmol, 1.49 g) in acetone (20 ml) was added hydrazine monohydrate (Sigma–Aldrich; 10 mmol, 0.76 ml). The resulting mixture was stirred for 4 h at room temperature. Both chloroform (20 ml) and acetonitrile (20 ml) were then added, and the resulting mixture left for slow evaporation. Light-brown crystals were obtained after 2 weeks. Yield: 2.012 g (91%). M.p. 412–413 K. ^{1}H NMR (400 MHz, $CDCl_3$, 298 K): 9.19 (*s*, *br*, 1H, NH—N), 8.56 (*s*, *br*, 1H, NH), 7.49 (*d*, 2H, *m*-aryl, J = 8.28 Hz), 7.17 (*d*, 2H, *o*-aryl, J = 8.24 Hz), 2.34 (*s*, 3H, aryl-CH_3), 2.05 (*s*, 3H, CH_3), 1.94 (*s*, 3H, CH_3). ^{13}C NMR (400 MHz, $CDCl_3$, 298 K): 176.4 [CS], 149.6 [$C(CH_3)_2$], 135.8 [C_{ipso}], 135.4 [C_{para}], 129.3 [C_{meta}], 124.5 [C_{ortho}], 25.3 [CH_3], 21.0 [aryl-CH_3], 16.9 [CH_3, *syn* to N—H]. IR (cm^{-1}): ν(N—H) 3240, 3168 (*m*), ν(C=N) 1514 (*vs*), ν(C—N) 1267 (*s*), ν(C=S) 1188 (*vs*).

7. Refinement

Crystal data, data collection and structure refinement details are summarized in Table 4. Carbon-bound H-atoms were placed in calculated positions (C—H = 0.95–0.98 Å) and were included in the refinement in the riding model approximation, with U_{iso}(H) set to 1.2–1.5U_{eq}(C). The N-bound H atoms were located in a difference Fourier map but were refined with a distance restraint of N—H = 0.88±0.01 Å, and with U_{iso}(H) set to 1.2U_{eq}(N).

Table 4
Experimental details.

Crystal data	
Chemical formula	$C_{11}H_{15}N_3S$
M_r	221.32
Crystal system, space group	Monoclinic, $P2_1/c$
Temperature (K)	100
a, b, c (Å)	13.7289 (13), 7.4341 (7), 11.5757 (11)
β (°)	102.690 (1)
V (Å^3)	1152.58 (19)
Z	4
Radiation type	Mo $K\alpha$
μ (mm^{-1})	0.25
Crystal size (mm)	0.12 × 0.05 × 0.03
Data collection	
Diffractometer	Bruker SMART APEX CCD
Absorption correction	Multi-scan (*SADABS*; Sheldrick, 1996)
T_{min}, T_{max}	0.970, 0.993
No. of measured, independent and observed [$I > 2\sigma(I)$] reflections	10739, 2646, 2052
R_{int}	0.050
(sin $\theta/\lambda)_{max}$ (Å^{-1})	0.650
Refinement	
$R[F^2 > 2\sigma(F^2)]$, $wR(F^2)$, S	0.041, 0.098, 1.02
No. of reflections	2646
No. of parameters	147
No. of restraints	2
H-atom treatment	H atoms treated by a mixture of independent and constrained refinement
$\Delta\rho_{max}$, $\Delta\rho_{min}$ (e Å^{-3})	0.27, −0.27

Computer programs: *APEX2* and *SAINT* (Bruker, 2008), *SHELXS97* (Sheldrick, 2008), *SHELXL2014*/7 (Sheldrick, 2015), *ORTEP-3 for Windows* (Farrugia, 2012), *QMol* (Gans & Shalloway, 2001), *DIAMOND* (Brandenburg, 2006) and *publCIF* (Westrip, 2010).

Acknowledgements

This research was supported by the Trans-disciplinary Research Grant Scheme (TR002-2014A) provided by the Ministry of Education, Malaysia. The intensity data set was provided by the University of Malaya Crystallographic Laboratory.

References

Bel'skii, V. K., Prisyazhnyuk, A. I., Kolchinskii, E. V. & Koksharova, T. V. (1987). *J. Struct. Chem.* **27**, 808–811.
Brandenburg, K. (2006). *DIAMOND*. Crystal Impact GbR, Bonn, Germany.
Bruker (2008). *APEX2* and *SAINT*. Bruker AXS Inc., Madison, Wisconsin, USA.
CambridgeSoft Corporation (2002). *CHEMDRAW Ultra*. Cambridge, USA.
Dessy, G., Fares, V., Scaramuzza, L., Tomlinson, A. A. B. & De Munno, G. (1978). *J. Chem. Soc. Dalton Trans.* pp. 1549–1554.
Dilworth, J. R. & Hueting, R. (2012). *Inorg. Chim. Acta*, **389**, 3–15.
Farrugia, L. J. (2012). *J. Appl. Cryst.* **45**, 849–854.
Gans, J. & Shalloway, D. (2001). *J. Mol. Graphics Modell.* **19**, 557–559.
Groom, C. R. & Allen, F. H. (2014). *Angew. Chem. Int. Ed.* **53**, 662–671.
Ho, S. Y., Bettens, R. P. A., Dakternieks, D., Duthie, A. & Tiekink, E. R. T. (2005). *CrystEngComm*, **7**, 682–689.
Ho, S. Y., Cheng, E. C.-C., Tiekink, E. R. T. & Yam, V. W.-W. (2006). *Inorg. Chem.* **45**, 8165–8174.

Jayatilaka, D., Grimwood, D. J., Lee, A., Lemay, A., Russel, A. J., Taylo, C., Wolff, S. K., Chenai, C. & Whitton, A. (2005). *TONTO – A System for Computational Chemistry*. Available at: http://hirshfeldsurface.net/

Jian, F.-F., Bai, Z.-S., Xiao, H.-L. & Li, K. (2005). *Acta Cryst.* E**61**, o653–o654.

Kuan, F. S., Yei Ho, S., Tadbuppa, P. P. & Tiekink, E. R. T. (2008). *CrystEngComm*, **10**, 548–564.

Lukmantara, A. Y., Kalinowski, D. S., Kumar, N. & Richardson, D. R. (2013). *Org. Biomol. Chem.* **11**, 6414–6425.

Ooi, K. K., Yeo, C. I., Ang, K.-P., Akim, A. Md., Cheah, Y.-K., Halim, S. N. A., Seng, H.-L. & Tiekink, E. R. T. (2015). *J. Biol. Inorg. Chem.* **20**, 855–873.

Rohl, A. L., Moret, M., Kaminsky, W., Claborn, K., McKinnon, J. J. & Kahr, B. (2008). *Cryst. Growth Des.* **8**, 4517–4525.

Sheldrick, G. M. (1996). *SADABS*. University of Göttingen, Germany.

Sheldrick, G. M. (2008). *Acta Cryst.* A**64**, 112–122.

Sheldrick, G. M. (2015). *Acta Cryst.* C**71**, 3–8.

Spackman, M. A. & Jayatilaka, D. (2009). *CrystEngComm*, **11**, 19–32.

Spackman, M. A., McKinnon, J. J. & Jayatilaka, D. (2008). *CrystEngComm*, **10**, 377–388.

Su, W., Qian, Q., Li, P., Lei, X., Xiao, Q., Huang, S., Huang, C. & Cui, J. (2013). *Inorg. Chem.* **52**, 12440–12449.

Venkatraman, R., Swesi, A. T. & Yamin, B. M. (2005). *Acta Cryst.* E**61**, o3914–o3916.

Westrip, S. P. (2010). *J. Appl. Cryst.* **43**, 920–925.

Wolff, S. K., Grimwood, D. J., McKinnon, J. J., Turner, M. J., Jayatilaka, D. & Spackman, M. A. (2012). *Crystal Explorer*. The University of Western Australia.

Yeo, C. I., Khoo, C.-H., Chu, W.-C., Chen, B.-J., Chu, P.-L., Sim, J.-H., Cheah, Y.-K., Ahmad, J., Halim, S. N. A., Seng, H.-L., Ng, S., Otero-de-la-Roza, A. & Tiekink, E. R. T. (2015). *RSC Adv.* **5**, 41401–41411.

Yeo, C. I., Ooi, K. K., Akim, A. Md., Ang, K. P., Fairuz, Z. A., Halim, S. N. B. A., Ng, S. W., Seng, H.-L. & Tiekink, E. R. T. (2013). *J. Inorg. Biochem.* **127**, 24–38.

Yeo, C. I., Sim, J.-H., Khoo, C.-H., Goh, Z.-J., Ang, K.-P., Cheah, Y.-K., Fairuz, Z. A., Halim, S. N. B. A., Ng, S. W., Seng, H.-L. & Tiekink, E. R. T. (2013). *Gold Bull.* **46**, 145–152.

Yeo, C. I., Tan, Y. S. & Tiekink, E. R. T. (2015). *Acta Cryst.* E**71**, 1159–1164.

Zhang, Y.-L., Wu, C.-Z. & Zhang, F.-J. (2011). *Acta Cryst.* E**67**, o1547.

supporting information

Acta Cryst. (2015). E**71**, 1236-1241 [doi:10.1107/S2056989015017624]

Crystal structure of 1-(4-methylphenyl)-3-(propan-2-ylideneamino)thiourea

Mukesh M. Jotani, Chien Ing Yeo and Edward R. T. Tiekink

Computing details

Data collection: *APEX2* (Bruker, 2008); cell refinement: *APEX2* (Bruker, 2008); data reduction: *SAINT* (Bruker, 2008); program(s) used to solve structure: *SHELXS97* (Sheldrick, 2008); program(s) used to refine structure: *SHELXL2014*/7 (Sheldrick, 2015); molecular graphics: *ORTEP-3 for Windows* (Farrugia, 2012), *QMol* (Gans & Shalloway, 2001), *DIAMOND* (Brandenburg, 2006); software used to prepare material for publication: *publCIF* (Westrip, 2010).

1-(4-Methylphenyl)-3-(propan-2-ylideneamino)thiourea

Crystal data

$C_{11}H_{15}N_3S$
$M_r = 221.32$
Monoclinic$P2_1/c$
$a = 13.7289$ (13) Å
$b = 7.4341$ (7) Å
$c = 11.5757$ (11) Å
$\beta = 102.690$ (1)°
$V = 1152.58$ (19) Å^3
$Z = 4$
$F(000) = 472$
$D_x = 1.275$ Mg m^{-3}
Mo $K\alpha$ radiation, $\lambda = 0.71073$ Å
Cell parameters from 1590 reflections
$\theta = 3.0$–25.5°
$\mu = 0.25$ mm^{-1}
$T = 100$ K
Prism, light-brown
0.12 × 0.05 × 0.03 mm

Data collection

Bruker SMART APEX CCD diffractometer
Radiation source: fine-focus sealed tube
Graphite monochromator
φ and ω scans
Absorption correction: multi-scan (*SADABS*; Sheldrick, 1996)
$T_{min} = 0.970$, $T_{max} = 0.993$
10739 measured reflections
2646 independent reflections
2052 reflections with $I > 2\sigma(I)$
$R_{int} = 0.050$
$\theta_{max} = 27.5°$, $\theta_{min} = 3.0°$
$h = -17\rightarrow17$
$k = -9\rightarrow9$
$l = -13\rightarrow15$

Refinement

Refinement on F^2
Least-squares matrix: full
$R[F^2 > 2\sigma(F^2)] = 0.041$
$wR(F^2) = 0.098$
$S = 1.02$
2646 reflections
147 parameters
2 restraints
Hydrogen site location: mixed
H atoms treated by a mixture of independent and constrained refinement
$w = 1/[\sigma^2(F_o^2) + (0.0332P)^2 + 0.7356P]$ where $P = (F_o^2 + 2F_c^2)/3$
$(\Delta/\sigma)_{max} < 0.001$
$\Delta\rho_{max} = 0.27$ e Å^{-3}
$\Delta\rho_{min} = -0.27$ e Å^{-3}

Special details

Geometry. All esds (except the esd in the dihedral angle between two l.s. planes) are estimated using the full covariance matrix. The cell esds are taken into account individually in the estimation of esds in distances, angles and torsion angles; correlations between esds in cell parameters are only used when they are defined by crystal symmetry. An approximate (isotropic) treatment of cell esds is used for estimating esds involving l.s. planes.

Fractional atomic coordinates and isotropic or equivalent isotropic displacement parameters (Å²)

	x	*y*	*z*	U_{iso}*/U_{eq}
S1	0.14991 (3)	0.10760 (6)	0.53754 (4)	0.01865 (13)
N1	0.17657 (11)	0.1754 (2)	0.31707 (14)	0.0179 (3)
H1N	0.1468 (14)	0.175 (3)	0.2419 (9)	0.023 (6)*
N2	0.01790 (11)	0.1178 (2)	0.33437 (14)	0.0174 (3)
H2N	−0.0236 (13)	0.073 (3)	0.3744 (17)	0.032 (6)*
N3	−0.00516 (11)	0.1118 (2)	0.21071 (13)	0.0177 (3)
C1	0.11491 (13)	0.1348 (2)	0.38949 (16)	0.0158 (4)
C2	0.28274 (13)	0.1793 (2)	0.34532 (16)	0.0174 (4)
C3	0.33249 (14)	0.0928 (3)	0.26883 (17)	0.0218 (4)
H3	0.2955	0.0313	0.2013	0.026*
C4	0.43587 (14)	0.0956 (3)	0.29054 (17)	0.0240 (4)
H4	0.4688	0.0357	0.2374	0.029*
C5	0.49234 (14)	0.1841 (3)	0.38822 (17)	0.0218 (4)
C6	0.44118 (15)	0.2713 (3)	0.46362 (18)	0.0240 (4)
H6	0.4781	0.3329	0.5311	0.029*
C7	0.33772 (14)	0.2703 (3)	0.44266 (17)	0.0221 (4)
H7	0.3046	0.3319	0.4949	0.027*
C8	0.60488 (15)	0.1844 (3)	0.4134 (2)	0.0316 (5)
H8A	0.6299	0.3006	0.4475	0.047*
H8B	0.6271	0.1650	0.3395	0.047*
H8C	0.6307	0.0880	0.4695	0.047*
C9	−0.09645 (13)	0.1333 (2)	0.15732 (16)	0.0163 (4)
C10	−0.18214 (14)	0.1717 (3)	0.21420 (17)	0.0220 (4)
H10A	−0.1571	0.2260	0.2922	0.033*
H10B	−0.2169	0.0592	0.2233	0.033*
H10C	−0.2285	0.2549	0.1643	0.033*
C11	−0.11855 (14)	0.1185 (3)	0.02523 (16)	0.0201 (4)
H11A	−0.0561	0.1262	−0.0024	0.030*
H11B	−0.1631	0.2166	−0.0096	0.030*
H11C	−0.1509	0.0028	0.0011	0.030*

Atomic displacement parameters (Å²)

	U^{11}	U^{22}	U^{33}	U^{12}	U^{13}	U^{23}
S1	0.0168 (2)	0.0218 (2)	0.0167 (2)	−0.00133 (19)	0.00219 (18)	0.00207 (18)
N1	0.0133 (8)	0.0252 (8)	0.0149 (8)	−0.0017 (6)	0.0020 (6)	0.0013 (7)
N2	0.0148 (8)	0.0226 (8)	0.0149 (8)	−0.0018 (6)	0.0033 (6)	0.0014 (6)
N3	0.0182 (8)	0.0196 (8)	0.0152 (8)	−0.0022 (6)	0.0037 (6)	0.0000 (6)
C1	0.0149 (9)	0.0129 (8)	0.0196 (9)	0.0003 (7)	0.0041 (7)	0.0007 (7)

C2	0.0151 (9)	0.0177 (8)	0.0194 (9)	−0.0003 (7)	0.0040 (7)	0.0046 (7)
C3	0.0200 (10)	0.0272 (10)	0.0181 (10)	−0.0009 (8)	0.0043 (8)	0.0008 (8)
C4	0.0194 (10)	0.0308 (11)	0.0239 (11)	0.0016 (8)	0.0092 (8)	0.0014 (8)
C5	0.0171 (10)	0.0233 (9)	0.0247 (10)	−0.0006 (8)	0.0038 (8)	0.0080 (8)
C6	0.0203 (10)	0.0258 (10)	0.0245 (11)	−0.0051 (8)	0.0018 (8)	−0.0010 (8)
C7	0.0206 (10)	0.0224 (9)	0.0251 (11)	−0.0026 (8)	0.0087 (8)	−0.0040 (8)
C8	0.0172 (10)	0.0364 (12)	0.0408 (13)	−0.0008 (9)	0.0053 (9)	0.0085 (10)
C9	0.0182 (9)	0.0121 (8)	0.0186 (9)	−0.0004 (7)	0.0041 (7)	0.0009 (7)
C10	0.0178 (10)	0.0288 (10)	0.0179 (10)	0.0056 (8)	0.0009 (8)	0.0009 (8)
C11	0.0199 (10)	0.0228 (9)	0.0167 (9)	−0.0008 (8)	0.0020 (8)	0.0004 (7)

Geometric parameters (Å, º)

S1—C1	1.6873 (18)	C5—C8	1.508 (3)
N1—C1	1.350 (2)	C6—C7	1.387 (3)
N1—C2	1.422 (2)	C6—H6	0.9500
N1—H1N	0.876 (9)	C7—H7	0.9500
N2—C1	1.350 (2)	C8—H8A	0.9800
N2—N3	1.397 (2)	C8—H8B	0.9800
N2—H2N	0.875 (9)	C8—H8C	0.9800
N3—C9	1.280 (2)	C9—C11	1.496 (2)
C2—C7	1.387 (3)	C9—C10	1.496 (3)
C2—C3	1.389 (3)	C10—H10A	0.9800
C3—C4	1.386 (3)	C10—H10B	0.9800
C3—H3	0.9500	C10—H10C	0.9800
C4—C5	1.388 (3)	C11—H11A	0.9800
C4—H4	0.9500	C11—H11B	0.9800
C5—C6	1.395 (3)	C11—H11C	0.9800
C1—N1—C2	127.79 (16)	C2—C7—C6	119.87 (18)
C1—N1—H1N	113.3 (14)	C2—C7—H7	120.1
C2—N1—H1N	117.3 (14)	C6—C7—H7	120.1
C1—N2—N3	117.72 (15)	C5—C8—H8A	109.5
C1—N2—H2N	118.4 (15)	C5—C8—H8B	109.5
N3—N2—H2N	120.2 (15)	H8A—C8—H8B	109.5
C9—N3—N2	117.91 (15)	C5—C8—H8C	109.5
N1—C1—N2	114.54 (16)	H8A—C8—H8C	109.5
N1—C1—S1	125.45 (14)	H8B—C8—H8C	109.5
N2—C1—S1	120.00 (14)	N3—C9—C11	116.21 (16)
C7—C2—C3	119.20 (17)	N3—C9—C10	126.34 (17)
C7—C2—N1	122.98 (17)	C11—C9—C10	117.46 (16)
C3—C2—N1	117.79 (17)	C9—C10—H10A	109.5
C4—C3—C2	120.30 (18)	C9—C10—H10B	109.5
C4—C3—H3	119.9	H10A—C10—H10B	109.5
C2—C3—H3	119.9	C9—C10—H10C	109.5
C3—C4—C5	121.42 (18)	H10A—C10—H10C	109.5
C3—C4—H4	119.3	H10B—C10—H10C	109.5
C5—C4—H4	119.3	C9—C11—H11A	109.5

C4—C5—C6	117.52 (17)	C9—C11—H11B	109.5
C4—C5—C8	121.55 (18)	H11A—C11—H11B	109.5
C6—C5—C8	120.92 (18)	C9—C11—H11C	109.5
C7—C6—C5	121.69 (18)	H11A—C11—H11C	109.5
C7—C6—H6	119.2	H11B—C11—H11C	109.5
C5—C6—H6	119.2		
C1—N2—N3—C9	−165.78 (16)	C3—C4—C5—C6	−0.4 (3)
C2—N1—C1—N2	−171.29 (17)	C3—C4—C5—C8	178.82 (19)
C2—N1—C1—S1	9.3 (3)	C4—C5—C6—C7	0.0 (3)
N3—N2—C1—N1	11.0 (2)	C8—C5—C6—C7	−179.16 (18)
N3—N2—C1—S1	−169.57 (12)	C3—C2—C7—C6	−1.1 (3)
C1—N1—C2—C7	−50.1 (3)	N1—C2—C7—C6	−178.81 (17)
C1—N1—C2—C3	132.2 (2)	C5—C6—C7—C2	0.7 (3)
C7—C2—C3—C4	0.8 (3)	N2—N3—C9—C11	−177.62 (15)
N1—C2—C3—C4	178.60 (17)	N2—N3—C9—C10	2.4 (3)
C2—C3—C4—C5	0.0 (3)		

Hydrogen-bond geometry (Å, º)

Cg1 is the centroid of the C2–C7 ring.

D—H···*A*	*D*—H	H···*A*	*D*···*A*	*D*—H···*A*
N1—H1*N*···N3	0.88 (1)	2.09 (2)	2.572 (2)	114 (1)
N1—H1*N*···S1^{i}	0.88 (1)	2.87 (2)	3.5618 (17)	137 (2)
N2—H2*N*···S1^{ii}	0.88 (2)	2.57 (2)	3.4373 (16)	169 (2)
C8—H8*C*···*Cg*1^{iii}	0.98	2.81	3.716 (2)	154

Symmetry codes: (i) *x*, −*y*+1/2, *z*−1/2; (ii) −*x*, −*y*, −*z*+1; (iii) −*x*+1, −*y*, −*z*+1.